ELSEVIER

Catalysis Today 38 (1997) 221–226

CATALYSIS TODAY

Mesoporous molecular sieve with binary transition metal (Zr–Cr) oxide framework

Ji Man Kim[a], Chae Ho Shin[b], Ryong Ryoo[a,*]

[a]*Department of Chemistry and Center for Molecular Science, Korea Advanced Institute of Science and Technology, Taejon 305-701, South Korea*

[b]*Catalysis Research Division, Korea Research Institute of Chemical Technology, Taejon 305-606, South Korea*

Abstract

A mesoporous molecular sieve with binary transition metal (Zr–Cr) oxide framework has been synthesized for the first time, and the material exhibits good thermal stability with a high surface area.

Keywords: Mesoporous molecular sieve; Zeolite; Binary trnasition; Zirconium oxide; Chromium oxide; Thermal stability; X-ray diffraction; Transition electron microscopy

1. Introduction

Recently, the templating route by surfactant micelle has led to the discovery of various kinds of large-pore molecular sieves constructed with silica frameworks such as MCM-41 [1,2], MCM-48 [1,2], FSM-16 [3], SBA-1, 2, 3 [4], HMS [5], MSU-1 [6], KIT-1 [7,8]. These molecular sieves have very large channels with 1.6–10 nm at the cross-section, compared with pore diameters of conventional microporous molecular sieves less than 1.5 nm. The pore diameter of the large-pore molecular sieves, which are called mesoporous molecular sieves, can be tailored within the 1.6–10 nm range by choosing surfactants with suitable chain length, using auxiliary organic additives during the hydrothermal crystallization process [1,2], and/or using post-synthesis wall-deposition and hydrothermal treatments [9]. The mesoporous molecular sieves attract much attention due to new possibilities of applications for adsorption, separation and catalytic conversion of large molecules which have difficulty entering conventional zeolite pores. Furthermore, the tailorability of the channel diameters provides a unique opportunity to tune the materials for specific uses.

However, the mesoporous molecular sieves constructed with silica frameworks are of limited use in catalysis, due to the lack of acidity and ion exchange sites. The acidity and ion exchange sites can be increased by incorporating aluminum into the siliceous frameworks [10,11]. The ion exchange capability of the materials on the 4-coordinated framework aluminum sites is useful for supporting catalytically active metal components [12], similar to conventional zeolites. The catalytic activity of the molecular sieves can also be promoted by incorporating transition metal elements such as Ti [5], Mn [13], Fe [14], V [15], etc. into the frameworks.

*Corresponding author. Fax: (82-42) 869-2810; e-mail: rryoo@sorak.kaist.ac.kr

PII S0920-5861(97)00069-2

Although more or less different mechanisms have been proposed for a synthetic route of the mesoporous molecular sieves [1–3,16–18], the synthesis is in general based on a cooperative formation of a periodic assembly between silicate and surfactant micelles. Huo et al. [19] reported that a similar nature of periodic assemblies can be formed between various transition metal oxides and organic surfactants. Various mesostructures based on tungsten, antimony, lead, iron, aluminum and zinc oxide and phosphate species were obtained using the surfactant–inorganic periodic assembly process. Many other studies also reported on the formation of mesostructures with various transition metal oxide or phosphate frameworks [20–26]. The surfactant–inorganic assemblies have either lamella or hexagonal structures, depending on the nature of the surfactants and the metal systems. In the case of the lamella structure, the structure always collapsed during calcination and/or solvent extraction, attempting to remove the surfactants from the mesostructures. In the case of the hexagonal structure, however, there were a few transition metal systems that maintained the structure after the removal of surfactants. Mesoporous transition metal oxides and phosphates thus obtained include titanium oxide [22], niobium oxide [23], zirconium oxide [24], oxophosphate [25], and tantalum oxide [26], etc. These recent reports highlight the syntheses of mesoporous molecular sieves with single-transition metal-based frameworks.

In the present work, we report on the synthesis and characterization of a mesoporous molecular sieve constructed with a zirconium–chromium mixed oxide framework. This new molecular sieve is the first example of a mesoporous molecular sieve constructed with binary transition metal system exhibiting sufficiently high thermal stability to be potentially useful for catalytic applications.

2. Experimental

A mesostructure with a zirconia-derivative framework was obtained through a hydrothermal synthesis using hexadecyltrimethylammonium (HTA) chloride, sulfuric acid and zirconyl nitrate. The initial gel mixture had a molar composition in the range of 1 HTACl : $x$$ZrO(NO_3)_2$: $y$$H_2SO_4$: $z$$H_2O$, where x=0.5–4, y=1–8 and z=150–300. The reaction mixture was heated at 370 K for 24 h. A 1 M aqueous solution of NaOH was added to the reaction mixture after cooling to room temperature. The mixture was heated again at 373 K for 24 h. A mesostructured product with a zirconium oxosulfate framework was collected from the reaction mixture by filtration and washed with doubly distilled water. The product was converted to oxophosphates by slurrying in aqueous solutions of phosphoric acid (0.01–0.1 M) at room temperature for 2 h. A zirconium oxochromate framework was also obtained by slurrying the oxosulfate product in Na_2CrO_4 solutions (0.01–0.1 M). Materials thus obtained were filtered, washed with doubly distilled water and dried in an oven at 373 K. The materials were calcined in air under static conditions using a muffle furnace. The calcination temperature was increased from room temperature to 813 K over 10 h and maintained at 813 K for 5 h.

The materials were investigated using X-ray powder diffraction (XRD), transmission electron microscopy (TEM) and gas adsorption. XRD patterns were obtained with a Cu K_α X-ray source using a Rigaku D/MAX-III (3 kW) instrument at room temperature. TEM images of thin edges of the sample were taken with a CM 20 (Philips) apparatus operating at 100 keV. Argon and N_2 physisorption measurements were conducted on an ASAP 2010 instrument at liquid argon and liquid N_2 temperatures, respectively. An elemental analysis was performed with inductively coupled plasma (ICP) emission spectroscopy (Shimadzu, ICPS-1000III).

3. Results and discussion

Fig. 1 shows XRD patterns of the zirconia-derivative mesostructures synthesized in the present work using aqueous solutions of HTACl, sulfuric acid and zirconyl nitrate. During the initial reaction period, a poorly defined XRD pattern was obtained (Fig. 1a). The XRD pattern could be due to the formation of a poorly ordered mesostructure, or a mixture of cubic and hexagonal mesophases. This mesostructure or mixture was transformed to a hexagonally ordered mesostructure by the addition of NaOH to the hydrothermal reaction mixture. The XRD patterns in Fig. 1b and c consist of one very intense line and two weak

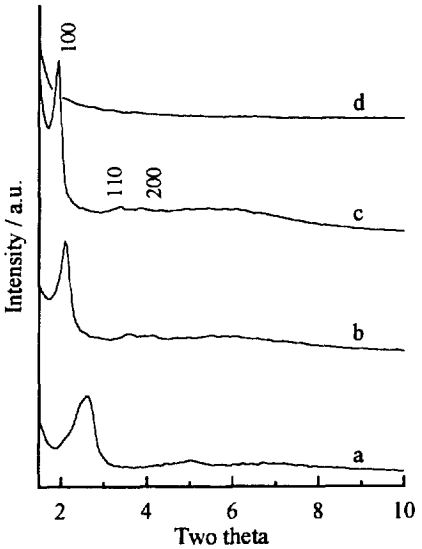

Fig. 1. XRD patterns of the surfactant–zirconium oxosulfate mesostructures obtained from hexadecyltrimethylammonium chloride–sulfuric acid–zirconyl nitrate–NaOH reaction mixtures. The ratios of $NaOH/SO_4^{2-}$ in the reaction mixtures were: (a) 0; (b) 1; (c) 2; and (d) more than 3, respectively.

lines, which can be indexed to (1 0 0), (1 1 0) and (2 0 0) diffraction lines characteristic of the hexagonal structure [1], respectively. Fig. 2 shows a TEM image obtained from the hexagonal sample presented in Fig. 1c. The TEM image has ordered lines with a spacing of 2.6 nm, which are expected when the sample is viewed along the (2 1 0) zone axis of the hexagonal cell with a unit cell dimension of a=5.1 nm. The unit cell dimension has been found to increase with increasing the $NaOH/SO_4^{2-}$ ratio from 0 to 2.5 for the reaction mixture. The addition of NaOH also led to a significant improvement in the textural uniformity. However, the mesostructure was lost when the pH was increased beyond 7 (Fig. 1d).

Elemental analysis of the hexagonal mesostructure indicated that the framework was constructed with zirconium oxosulfate with S/Zr=1. The structure collapsed upon calcination in air under static conditions at 813 K in order to remove the surfactant. The sulfur content decreased to S/Zr<0.05 during the calcination. The structure collapse corresponded to the transformation of the zirconium oxosulfate framework to zirconium oxide, due to the oxosulfate decomposition.

Sulfate in the mesostructure framework was substituted with phosphate when the surfactant–zirco-

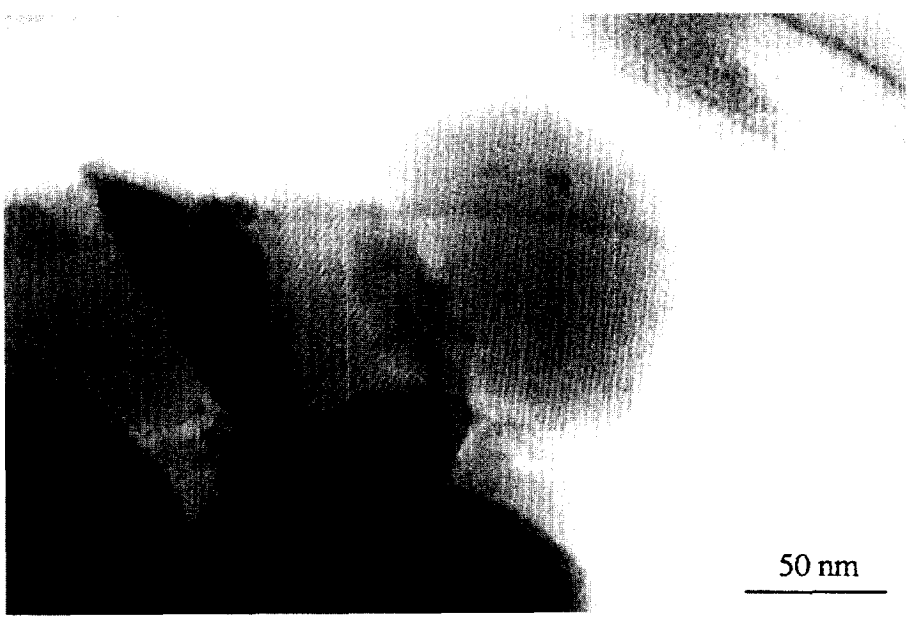

Fig. 2. Transmission electron micrographic image of the hexadecyltrimethylammonium–zirconium oxosulfate mesostructure presented in Fig. 1c.

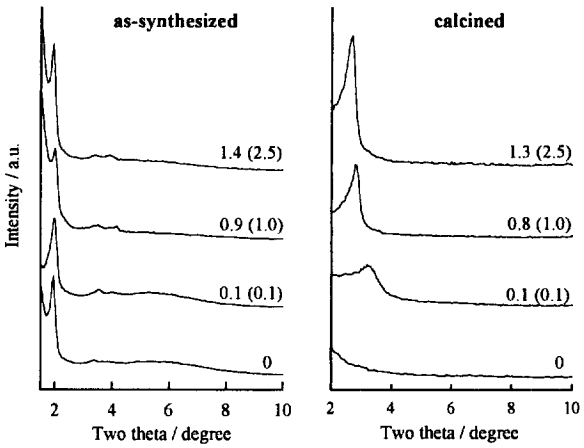

Fig. 3. X-ray powder diffraction patterns of the mesostructures constructed with zirconium oxophosphate frameworks. Calcination was performed in air under static conditions at 813 K for 5 h. The zirconium oxosulfate mesostructures were obtained by slurrying the hexadecyltrimethylammonium–zirconium oxosulfate (S/Zr=1) mesostructure in aqueous solutions of phosphoric acid. Numbers before parentheses indicate ratios of P/Zr in the mesostructures. Numbers in the parentheses are the ratios used for the sample preparation, i.e., molar ratios of phosphoric acid used per Zr.

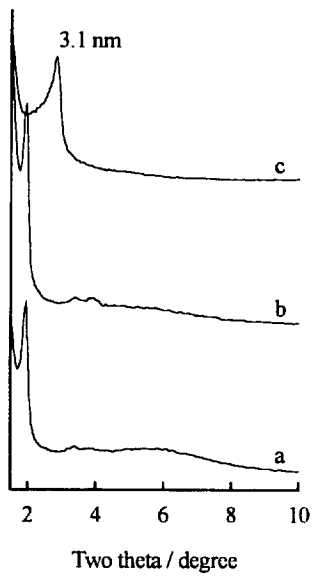

Fig. 4. X-ray powder diffraction patterns: (a) hexadecyltrimethylammonium (HTA)–zirconium oxosulfate mesostructure; (b) HTA–zirconium oxochromate mesostructure before calcination; and (c) the same HTA–zirconium oxochromate mesostructure after calcination in air under static conditions at 813 K for 5 h. The HTA–zirconium oxochromate mesostructure was obtained by slurrying the oxosulfate mesostructure in an aqueous solution of Na_2CrO_4.

nium oxosulfate (S/Zr=1) was slurried in aqueous solutions of phosphoric acid. The P/Zr ratios shown in Fig. 3 indicate that the substitution with phosphate was almost limited by the amount of phosphoric acid used in the solution. Almost all the used phosphate was incorporated into the framework, substituting the sulfate, when relatively small amounts of phosphoric acid were used compared with the number of sulfate moles. As the amounts of the phosphoric acid increased to much more than the number of the sulfate moles present in the initial oxosulfate mesostructure, the framework was completely transformed into zirconium oxophosphate and the P/Zr ratio in the framework increased to above 1 as shown in Fig. 3d. The oxophosphate frameworks did not collapse during the surfactant removal by calcination at 813 K, unlike the case of the oxosulfate mesostructure. Consequently, the calcined materials showed XRD patterns with a peak at low angles below $2\theta=4^\circ$. The intensity of the XRD peak increased as the P/Zr ratios in the frameworks increased within the range up to 1.4 investigated in the present work. The d_{100} spacing also increased with the P/Zr ratios. However, the higher order diffraction lines disappeared during calcination, indicating a significant loss of structural uniformity. In spite of the loss in the structural order, specific BET surface areas as high as 280 $m^2\ g^{-1}$ could be obtained using N_2 adsorption for the zirconium oxophosphate mesostructure presented in Fig. 3d. It is remarkable that the thermal stability of the zirconium oxosulfate mesostructure was increased by the substitution of the sulfate with phosphate, which is in good agreement with the previous report by Ciesla et al. [25].

Sulfate in the mesostructure framework was also substituted with chromate when the surfactant–zirconium oxosulfate (S/Zr=1) was slurried in aqueous solutions of Na_2CrO_4 (Fig. 4). The degree of substitution was able to be controlled up to Cr/Zr=1.2 by the amounts of the chromate solution, similar to the substitution of phosphate. The hexagonal mesostructure was maintained after the substitution with chromate. XRD patterns showed that d_{100} spacing increased slightly due to the chromate substitution. The resulting oxochromate materials were able to be calcined without collapsing the frameworks at 813 K for 5 h, similar to the oxophosphate mesostructures.

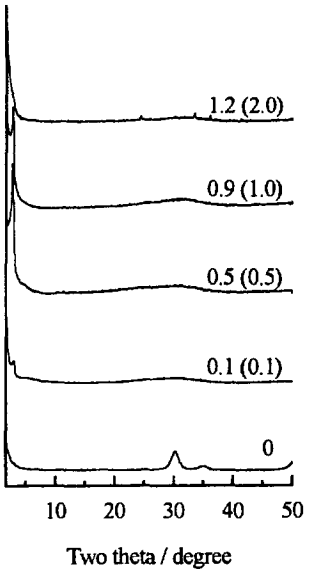

Fig. 5. X-ray powder diffraction patterns of zirconium–chromium binary oxide materials obtained after calcination of hexadecyltrimethylammonium–zirconium oxochromate mesostructures in air under static conditions at 813 K for 5 h. Numbers before parentheses indicate the Cr/Zr ratios for the calcined samples. Numbers in the parentheses denote molar ratios of Na_2CrO_4 used per Zr.

XRD patterns obtained after calcination indicated that thermal stability of the chromate-substituted frameworks increased as the Cr/Zr ratio increased to 0.5 (Fig. 5). However, the stability decreased with further increases in the Cr/Zr ratio. When the Cr/Zr ratio was 1.2, calcined material had XRD lines indicating the formation of extraframework metal oxides. The specific BET surface area of the calcined material with Cr/Zr=0.5 was 374 $m^2 g^{-1}$. Elemental analysis revealed that the framework was constructed with zirconium–chromium binary oxide.

Fig. 6 shows argon adsorption and desorption isotherms for the zirconium–chromium binary oxide material with Cr/Zr=0.5 obtained after calcination in air at 813 K. A small stepwise increase appeared in the adsorption isotherm around P/P_0=0.1, indicating capillary condensation in mesopores. No hysteresis loop was obtained. The total pore volume of this mesoporous material was 0.18 $cm^3 g^{-1}$. A Horvath–Kawazoe plot [27] of the argon adsorption for the mesostructure indicated that the material had two kinds of pores. The pore size (0.7 nm) of one was

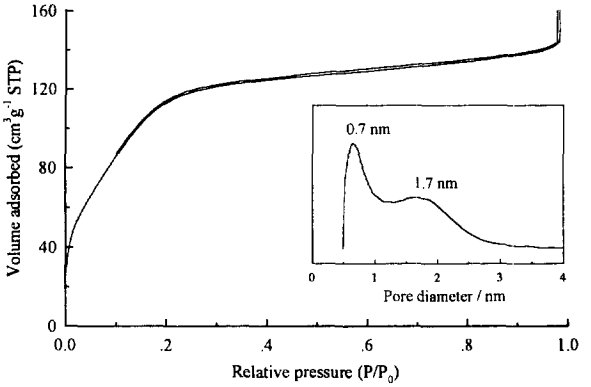

Fig. 6. Argon adsorption and desorption isotherms for a mesoporous molecular sieve constructed with a zirconium–chromium binary oxide (Cr/Zr=0.5) framework, after calcination in air under static conditions at 813 K. Inset, the corresponding pore size distribution curve obtained by the Horvath–Kawazoe analysis [27].

in the microporous range, and the other (1.7 nm) was in the mesoporous range. The pore size distribution for the material is very similar to that of MCM-41 with a somewhat poor structural order [10]. Therefore, the material can be regarded as a mesoporous molecular sieve with a framework constructed with zirconium oxide and chromium oxide.

In summary, a mesoporous molecular sieve with a binary transition metal (zirconium–chromium) oxide framework has been synthesized for the first time. The present material exhibited a high surface area with good thermal stability. Considering the significance of zirconia and chromia as catalytic materials, it will be interesting to explore the catalytic activity of the present mesoporous molecular sieve.

References

[1] C.T. Kresge, M.E. Leonowicz, W.J. Roth, J.C. Vartuli and J.S. Beck, Nature, 359 (1992) 710.
[2] J.S. Beck, J.C. Vartuli, W.J. Roth, M.E. Leonowicz, C.T. Kresge, K.D. Schmitt, C.T.-W. Chu, D.H. Olson, E.W. Sheppard, S.B. McCullen, J.B. Higgins and J.L. Schlenker, J. Am. Chem. Soc., 114 (1992) 10834.
[3] S. Inagaki, Y. Fukushima and K. Kuroda, J. Chem. Soc., Chem. Commun., (1993) 680.
[4] Q. Huo, R. Leon, P.M. Petroff and G.D. Stucky, Science, 268 (1995) 1324.
[5] P.T. Tanev, M. Chibwe and T.J. Pinnavaia, Nature, 368 (1994) 321.

[6] S.A. Bagshaw, E. Prouzet and T.J. Pinnavaia, Science, 269 (1995) 1242.
[7] R. Ryoo, J.M. Kim, C.H. Shin, J.Y. Lee, Proceedings of the 11th International Zeolite Conference, 1996.
[8] R. Ryoo, J.M. Kim, C.H. Ko and C.H. Shin, J. Phys. Chem., 100 (1996) 17718.
[9] Q. Huo, D.I. Margolese and G.D. Stucky, Chem. Mater., 8 (1996) 1147.
[10] A. Corma, V. Fornés, M.T. Navarro and J. Pérez-Pariente, J. Catal., 148 (1994) 569.
[11] J.M. Kim, J.H. Kwak, S. Jun and R. Ryoo, J. Phys. Chem., 99 (1995) 16742.
[12] R. Ryoo, C.H. Ko, J.M. Kim and R. Howe, Catal. Lett., 37 (1996) 29.
[13] D. Zhao and D. Goldfarb, J. Chem. Soc., Chem. Commun., (1995) 875.
[14] A. Tuel and S. Gontier, Chem. Mater., 8 (1996) 114.
[15] K.M. Reddy, I. Moudrakovski and A. Sayari, J. Chem. Soc., Chem. Commun., (1994) 1059.
[16] A. Monnier, F. Schüth, Q. Huo, D. Kumar, D. Margolese, R.S. Maxwell, G.D. Stucky, M. Krishnamurty, P. Petroff, A. Firouzi, M. Janicke and B.F. Chmelka, Science, 261 (1993) 1299.
[17] C.-Y. Chen, S.L. Burkette, H.-X. Li and M.E. Davis, Microporous Mater., 2 (1993) 27.
[18] P. Behrens, Angew. Chem. Int. Ed. Engl., 35 (1996) 515.
[19] Q. Huo, D.I. Margolese, U. Ciesla, P. Feng, T.E. Gier, P. Sieger, R. Leon, P.M. Petroff, F. Schüth and G.D. Stucky, Nature, 368 (1994) 317.
[20] T. Abe, A. Taguchi and M. Iwamoto, Chem. Mater., 7 (1995) 1429.
[21] V. Luca, D.J. MacLachlan, J.M. Hook and R. Withers, Chem. Mater., 7 (1995) 2220.
[22] D.M. Antonelli and J.Y. Ying, Angew. Chem. Int. Ed. Engl., 34 (1995) 2014.
[23] D.M. Antonelli and J.Y. Ying, Angew. Chem. Int. Ed. Engl., 35 (1996) 426.
[24] J.A. Knowles and M.J. Hudson, J. Chem. Soc., Chem. Commun., (1995) 2083.
[25] U. Ciesla, S. Schacht, G.D. Stucky, K.K. Unger and F. Schüth, Angew. Chem. Int. Ed. Engl., 35 (1996) 541.
[26] D.M. Antonelli and J.Y. Ying, Chem. Mater., 8 (1996) 874.
[27] G. Horváth and K. Kawazoe, J. Chem. Eng. Jpn., 16 (1983) 470.